



Holocene black carbon in New Zealand lake sediment records



Sandra O. Brugger ^{a,b,c,d,*}, David B. McWethy ^d, Nathan J. Chellman ^c, Matiu Prebble ^{e,f}, Colin J. Courtney Mustaphi ^a, Sabine Eckhardt ^g, Andreas Plach ^h, Andreas Stohl ^h, Janet M. Wilmshurst ⁱ, Joseph R. McConnell ^c, Cathy Whitlock ^d

^a University of Basel, Switzerland

^b Paul Scherrer Institute, Switzerland

^c Desert Research Institute, USA

^d Montana State University Bozeman, USA

^e University of Canterbury, New Zealand

^f Australian National University, Australia

^g NILU, Norway

^h University of Vienna, Austria

ⁱ Manaaki Whenua-Landcare Research, New Zealand

ARTICLE INFO

Handling Editor: Dr Yan Zhao

Keywords:

Biomass burning aerosols

Combustion products

Fire emissions

Holocene

Organic geochemistry

Paleofire

Paleolimnology

Refractory black carbon (rBC)

Southern Ocean

ABSTRACT

Black carbon emitted from incomplete combustion of biomass and fossil fuel burning is an important aerosol; however, available long-term black carbon data are limited to remote polar and high-alpine ice cores from few geographic regions. Black carbon records from lake sediments fill geographic gaps but such records are still scarce, particularly in the Southern Hemisphere. We applied a new incandescence-based methodology to develop Holocene refractory black carbon (rBC) records from four lake-sediment archives in New Zealand and compare these with macroscopic charcoal records. Our rBC records suggest periods with substantial rBC deposition during the Holocene before human arrival in the 13th century reflecting long-range transport and possibly local wetland fires. With Polynesian settlement, rBC deposition increased on the South Island in agreement with macroscopic charcoal records, and it is this period of burning that is proposed as the source of rBC increases evident in Antarctic ice cores. However, sites on the North Island show no contemporaneous rBC increase suggesting regional differences in biomass burning patterns between the North and South islands. None of the New Zealand records show an increase in rBC from fossil fuel sources during the Industrial Era post-1850 CE.

1. Introduction

Prior to the Industrial Revolution, humans directly and indirectly changed the global climate system through burning and associated aerosol emissions (Bond et al., 2013). Fires release many compounds that range from macroscopic-size solid burnt fragments to fine aerosols and greenhouse gases that affect human health, infrastructure, and ecosystems and induce climate feedbacks at local to global scales (Andreae and Merlet, 2001; Watts and Brugger, 2022). For example, black carbon from incomplete combustion is an important aerosol that modifies atmospheric conditions through light absorption and as cloud

condensation nuclei that alter cloud properties (Hartmann et al., 2019; Motos et al., 2019; Chatterjee et al., 2020). The insufficient understanding of black carbon and other biomass-burning emissions into the atmosphere results in uncertainties about the role of fire-created aerosols in climate models (Hamilton et al., 2018; Liu et al., 2021; Eckhardt et al., 2023).

In addition to biomass burning, fossil-fuel combustion has contributed significantly to black carbon emissions in recent centuries (Novakov et al., 2003; Sigl et al., 2018). To date, reconstructions of black carbon emissions during the Pre-industrial and Industrial eras are based mainly on data from remote polar and high-alpine ice cores (e.g.,

* Corresponding author. University of Basel, Switzerland.

E-mail addresses: sandra.bruegger@unibas.ch (S.O. Brugger), dmcwethy@montana.edu (D.B. McWethy), Nathan.chellman@dri.edu (N.J. Chellman), matiu.prebble@canterbury.ac.nz (M. Prebble), colin.courtney-mustaphi@unibas.ch (C.J. Courtney Mustaphi), sec@nilu.no (S. Eckhardt), andreas.plach@univie.ac.at (A. Plach), andreas.stohl@univie.ac.at (A. Stohl), WilmshurstJ@landcareresearch.co.nz (J.M. Wilmshurst), joe.mcconnell@dri.edu (J.R. McConnell), whitlock@montana.edu (C. Whitlock).

McConnell et al., 2007, 2021; Arienzo et al., 2017; Osmont et al., 2018, 2019; Brugger et al., 2022). Black carbon preserved in lake sediments could broaden the geographic coverage of information on biomass burning, but few lake sediment black carbon records have been developed to date using a variety of methods that measure different parts of the black carbon continuum (Arienzo et al., 2019; Gustafsson et al., 2001; Han et al., 2011; Ruppel et al., 2021). This sparsity of black carbon data limits our understanding of regional black-carbon deposition, specifically at low and mid latitudes such as in New Zealand, where the arrival of Polynesians in New Zealand in the 13th century (Wilmshurst et al., 2008; Bunbury et al., 2022) was accompanied by an unprecedented increase in fire activity and loss of large areas of native forests (McWethy et al., 2009, 2010; Perry et al., 2014).

This transformation is registered by macroscopic charcoal and pollen records from the sediments of small lakes and wetlands (McGlove and Wilmshurst, 1999; Perry et al., 2014). Although Antarctic ice-core records show an increase in black carbon deposition after 1200 CE (Fig. 1; McConnell et al., 2021), contemporaneous with the charcoal increase in the South Island of New Zealand, quantitatively linking charcoal and black carbon records from the two locations is challenging for several reasons (Newnham, 2022). First, there are several inherent differences between paleofire reconstructions based on macroscopic charcoal particles in lake sediments and black carbon. Macroscopic charcoal records reflect burning at local and landscape scales due to the large size of macroscopic charcoal (>125 µm in particle diameter; Whitlock and Millspaugh, 1996; Adolf et al., 2018; Whitlock and Larsen, 2002), whereas black carbon aerosols of <0.5 µm may be transported thousands of kilometers (Liu et al., 2021). Second, composites of macroscopic charcoal-based fire reconstructions show more temporal and spatial variability than single large-scale reconstructions of black carbon due to the chronological and sampling precision in lake sediment records; the complexity of local charcoal source areas; and the uneven spatial distribution, limited transport, and deposition of macroscopic charcoal (Marlon, 2020).

Macroscopic charcoal data from a cultivated wetland in the northern North Island show that changes in cultivation strategy during the different periods of human settlement, identified from pollen and archaeobotanical findings, resulted in highly contrasting levels of charcoal deposition from extremely high during initial human settlement to very low in later settlement periods (Prebble et al., 2019). This record contrasts with subalpine lake records from the southern South Island, remote from human settlements identified in the archeological

record, which reveal an order of magnitude less charcoal deposition, but provide records reflecting broader patterns of wildfires (McWethy et al., 2014). Black carbon and charcoal data from the same sites have the potential to clarify changes in black carbon production, transport, and deposition in the context of local fire history. Such insights help resolve recent controversies concerning the interpretation of black-carbon records in Antarctic ice cores and their potential source in New Zealand (McConnell et al., 2021; Newnham, 2022).

In this study, we used an incandescence-based methodology with a Single Particle Soot Photometer (SP2) instrument (Chellman et al., 2018) to measure refractory black carbon (rBC) from sediment cores from four small lakes in different environmental settings on the North and South Islands of New Zealand. Our objectives in this paper are to: (1) reconstruct trends in rBC deposition over the Holocene; (2) assess levels of rBC deposition before and after initial human arrival; (3) compare rBC levels from fossil fuel sources during the Industrial Era with Holocene background levels; and (4) provide a possible connection between source emissions and deposition in remote ice archives. Such data improve our ability to incorporate black-carbon emission data in global climate and biosphere models (Van Marle et al., 2017; F. Li et al., 2019).

2. Regional setting

New Zealand consists of two main islands (the South Island and North Island) with many offshore islands, with a maximum elevation of 3754 m a.s.l. at Aoraki Mount Cook. Generally, the climate of New Zealand is characterized by mild winters and moderately warm summers. Annual precipitation is between 970 mm y⁻¹ on the South Island site Horseshoe Lake and up to 1500 mm y⁻¹ at Lake Kai Iwi on the coast of the North Island. The South Island lies within the cool sub-polar westerly circulation between 40 and 60°S which is modulated by the Southern Annular Mode (SAM) influencing regional rainfall and temperature in the mid-latitudes of the southern hemisphere (Hinojosa et al., 2017; Sturman et al., 1984). FLEXPART atmospheric transport model simulations show that air masses entrained in the Southern Westerlies commonly reach the South Island and travel long distances over the Southern Ocean (McConnell et al., 2021) (Fig. 1). On the other hand, the North Island receives warm maritime air from the subtropical Pacific (Shulmeister et al., 2004). These differences in wind patterns and precipitation in New Zealand may influence rBC deposition on South and North Island from long-distance sources such as mainland Australia. During most of the Holocene, New Zealand was almost entirely forested, dominated by closed canopy evergreen angiosperm and conifer forests (Wood et al., 2017), and fires were infrequent (McWethy et al., 2010; Perry et al., 2014).

The four study lakes (Fig. 1) span a latitudinal and longitudinal gradient across New Zealand from 45°S to 36°S and 168°E to 175°E and an altitude range from sea level to 460 m a.s.l. elevation (Table 1). Diamond Lake (44.6°S and 168.9°E) is a mid-elevation site near Lake Wānaka on the South Island and located at an elevation of 395 m a.s.l. (Fig. 1). Previous research at the site examined multiple proxy records to infer the environmental history (e.g., Argiridis et al., 2018; McWethy et al., 2010). A macroscopic charcoal-derived fire-history reconstruction suggests southern beech forests rarely burned before the arrival of humans. A dramatic increase in fire activity during the Early Māori period from 1320 to 1560 CE was associated with the transition of closed-canopy beech forests to open grasslands mixed with *Leptospermum* scrub, bracken fern (*Pteridium*), and small trees (McWethy et al., 2010). Horseshoe Lake (42.6°S and 172.5°E), another mid-elevation site (460 m a.s.l.), is located in the central foothills of the South Island (Fig. 1). Pollen, charcoal, and geochemical records reveal a rapid transformation from closed-canopy forest to the current mosaic of open grassland, *Leptospermum* scrub, and bracken fern vegetation around 1370 CE (McWethy et al., 2010). The vegetation transformation was accompanied by significant fire activity that increased local erosion in subsequent centuries (McWethy et al., 2010).

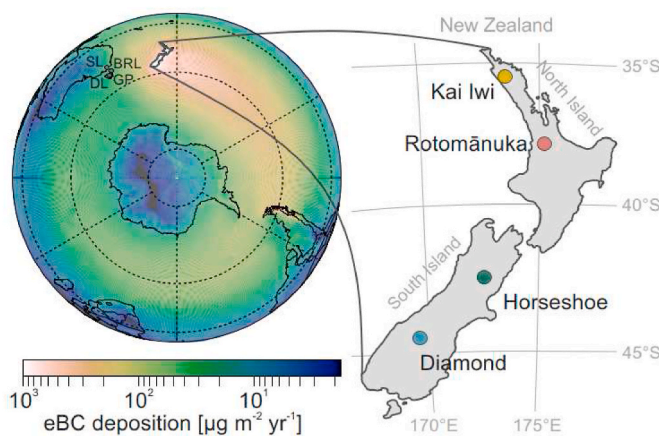


Fig. 1. Map of Southern Hemisphere and study region showing FLEXPART atmospheric aerosol deposition fluxes obtained from a forward simulation (Stohl et al., 2005; Pisso et al., 2019) for equivalent black carbon (eBC) emissions from New Zealand. Selected charcoal sites are shown for comparison (Gray circles; DL = Dove Lake; GP = Granta Pool; BRL = Big Reedy Lagoon; SL = Swallow Lagoon). Right panel shows zoom of New Zealand with location of the four lake sites across the South and North Island.

Table 1

Information on sediment cores. Last column shows number of rBC (refractory black carbon) samples [N], replicates [R] and duplicates [D]. Precipitation data from [Leathwick et al. \(2003\)](#).

Site name	Location	Elevation [m a.s.l.]	Precipitation [mm yr ⁻¹]	Modern vegetation	Chronology	Charcoal data	rBC samples [N, R, D]
Diamond Lake	44.65°S 168.96°E	395	1004	Grassland mixed with small trees, <i>Leptospermum</i> scrub, and bracken fern	McWethy et al. (2010)	McWethy et al. (2010)	N = 573 D = 29 R = 34
Horseshoe Lake	42.59°S 172.52°E	460	969	Grassland mixed with small trees, <i>Leptospermum</i> scrub, and bracken fern	McWethy et al. (2010)	McWethy et al. (2010)	N = 112 D = 9 R = 5
Lake Rotomānuka	37.926°S 175.32°E	58	1211	Improved pasture	See Appendix A	See Appendix A	N = 151 D = 17 R = 8
Lake Kai Iwi	35.81°S 173.65°E	76	1491	Grassland mixed with small trees, <i>Leptospermum</i> scrub, and bracken fern	See Appendix A	See Appendix A	N = 151 D = 14 R = 13

Lake Rotomānuka (37.9°S and 175.3°E) is a low-elevation site (58 m a.s.l.) on the North Island located ~12 km south of Hamilton (Fig. 1). The lake is a remnant of a former larger lake and peatland complex that was drained in the 20th century to a present-day surface area of about 12 ha ([Newnham et al., 1989](#)). *Nothofagus* and *Podocarpus* forests around Lake Rotomānuka were converted to open grassland and bracken fern scrubland with the arrival of early Polynesians in the 14th century, similar to the South Island sites. The transformation was accompanied by an increase in fire activity in the area although sediment chronology uncertainties limit a better constrained timing of initial burning at this site ([Newnham et al., 1989](#)). Large areas around Lake Rotomānuka are now used for improved pasture and other agricultural purposes. Lake Kai Iwi (35.8°S and 173.7°E), the northernmost site in this study, is a coastal lake (76 m a.s.l.) along the Northland Peninsula of the North Island (Fig. 1). The lake is part of the Kai Iwi lake complex of the coastal dune belt ([Newnham et al., 2017](#)). The current vegetation is composed of open grassland mixed with *Leptospermum* scrub, bracken fern, and small trees. This study presents the first multi-millennial fire history for the Lake Kai Iwi catchment.

3. Materials and methods

3.1. Sediment chronologies and macroscopic charcoal data

Sediment cores from Diamond Lake and Horseshoe Lake are 573 cm and 112 cm long, respectively, and the chronologies, based on radiocarbon dates of terrestrial macrofossils, reveal a ~14,500 year-long record for Diamond Lake and a ~920 year-long record for Horseshoe lake ([McWethy et al., 2010](#)).

The sediment cores from Lake Rotomānuka and Lake Kai Iwi were 150 cm and 153 cm in length. The chronologies were based on radiocarbon dates of terrestrial macrofossils. Details on the chronologies for both sites are provided in the supplementary material ([Appendix A](#); [Appendix C Table S1](#) and [Fig. S1](#)). The Lake Rotomānuka sediment core spans the last ~6600 years and two radiocarbon dates were used to develop the age-depth chronology. The Lake Kai Iwi record spans the last ~14,800 years and shows a relatively slow and constant sediment accumulation rate for the entire core. Macroscopic charcoal analyses for both sites on the North Island followed the same methodology as for the South Island cores ([McWethy et al., 2010](#), [Whitlock and Larsen, 2002](#)) with contiguous 1-cm sampling resolution, see supplementary material for details on the methods. All derived sediment ages are presented as calibrated years before 1950 CE (cal yr BP), calibrated with the SHCal20 calibration curve ([Hogg et al., 2020](#)).

3.2. rBC analyses

The Single-Particle Soot Photometer (SP2) instrument is sensitive to highly condensed, sub-micron diameter soot particles typically referred

to as refractory black carbon (rBC). The SP2 has been used extensively to measure rBC in the atmosphere ([Schwarz et al., 2008](#)), water ([Ohata et al., 2013](#); [Kruger et al., 2023](#)), snow samples ([Schwarz et al., 2013](#); [Osmont et al., 2020](#)), ice cores (e.g., [Arienzo et al., 2017](#); [Brugger et al., 2022](#); [McConnell et al., 2007, 2021](#); [Osmont et al., 2018](#)), and more recently the instrument has been adapted for lake sediments ([Chellman et al., 2018](#); [Arienzo et al., 2019](#)), specifically for paleofire reconstructions ([Li et al., 2019](#)). For the rBC measurements, the sediment cores from Diamond Lake, Horseshoe Lake, Lake Rotomānuka and Lake Kai Iwi were sampled contiguously at 1-cm depth resolution for direct comparison with the macroscopic charcoal data ([Table 1](#)). Additionally, between 5 and 8% of the depth units for each sediment core were subsampled in duplicate [D] to assess the reproducibility of the measurements. rBC analyses followed the methods described in [Chellman et al. \(2018\)](#). The samples were first dried and homogenized using a planetary ball mill. About 50 mg of dried sediment was suspended in 50 ml ultrapure water (18.2 MΩ) in a pre-cleaned polypropylene vial. Sediment and water weights were used to determine the exact ratio of sediment mass (mg) to water volume (ml) in order to calculate final rBC concentrations (μg BC g sediment⁻¹). Samples were subsequently shaken and sonicated vigorously to mobilize the rBC from the sediment matrix before storage for 24 h at 10 °C to settle out the larger sediment particles ([Chellman et al., 2018](#)).

To measure rBC, the aqueous samples passed through 20 and 10 μm stainless steel inline filters before introducing them to an Apex-Q nebulizer that aerosolized the liquid sample. The dry aerosol was sent to the SP2 to measure rBC concentrations. Potential iron oxide interferences were corrected by using the ratio of the narrow and wide-band SP2 channels. Aqueous standards made from black carbon-like materials (Cabojet 200, Aquadag, and Regal Black) were measured routinely at the beginning and end of each analysis day as well as throughout the analysis run for calibration. About 5% of the rBC samples were reanalyzed at the end of each measurement day (called replicate samples [R], [Table 1](#)) to assess rBC settling and instrument drift during a set of samples. See [Chellman et al. \(2018\)](#) for further description of the internal calibration procedure of the SP2 instrument.

rBC concentrations were converted to rBC influx (deposition) per time in a given area (μg cm⁻² y⁻¹) using an estimated sediment density of 0.3 g cm⁻³, a conservative estimate derived from other New Zealand sediments ([Page et al., 1994](#); [Pearson, 2007](#)) and calculated sediment accumulation rates. rBC influx is preferred to concentration data for interpreting fire activity because it accounts for variations in sediment accumulation rates over time and between different sites. rBC influx was examined for four periods: the pre-human period of the last millennium (1000 cal yr BP to 670 cal yr BP), the Early Māori period (670–350 cal yr BP), the Late Māori period (350–110 cal yr BP), and the Industrial period (110 cal yr BP to modern), by calculating boxplots that included all samples of an individual site and the mid-age for each of the respective periods. Only one sample measurement was included for each sample

depth unit, thereby excluding all the duplicate and replicate measurements.

4. Results

4.1. Accuracy of rBC measurements

rBC concentrations in the original, replicate, and duplicate samples from all four lakes ranged from below detection limit ($<2.1 \mu\text{g g}^{-1}$) up to $400 \mu\text{g g}^{-1}$. Replicate measurements revealed similar concentrations compared to the initial measurements ($r = 0.99$; Figs. 2–5; Appendix C; Fig. S2). The measured concentrations in independent duplicate subsamples were within an acceptable statistical range of the original samples ($r = 0.63$), although duplicate measurements showed more variability compared to the replicate measurements. For example, the original and duplicate measurements in the Lake Rotomānuka sediment core for the period from ~ 2500 – ~ 1500 cal yr BP and in the topmost sediment section were below the detection limit of rBC concentrations; these values close to zero resulted in comparatively large percentage variability among samples (Fig. 4). The original and duplicate samples at ~ 5500 cal yr BP, ~ 1400 cal yr BP, and ~ 800 cal yr BP in the Lake Rotomānuka record came from sections with high rBC concentrations ($\sim 60 \mu\text{g g}^{-1}$), and duplicate measurement closely matched the original sample concentrations ($r = 0.70$). Likewise, the original and duplicate samples from Lake Diamond (0.59), Lake Horseshoe (0.66), and Lake Kai Iwi (0.85) were correlated even though they came from independent sediment samples of the same depth. Together, the 60 replicate and 69 duplicate pairs from all four lake-sediment cores confirmed the accuracy and robustness of this relatively new methodology for rBC measurements in lake sediments (Chellman et al., 2018).

4.2. Holocene rBC trends from individual sites and comparison with charcoal data

The rBC record from Diamond Lake on the South Island spans the last $\sim 14,500$ years with concentrations reaching up to $400 \mu\text{g g}^{-1}$ (Fig. 2). Influx was overall low with values only reaching $4 \mu\text{g cm}^{-2} \text{y}^{-1}$ in contrast to the high concentration values. Trends in rBC influx and concentrations were highly correlated ($r = 0.97$ for samples before 4000 cal yr BP), except for the last ~ 4000 years when rBC influx increased relative to the concentration values as a result of the decreasing sedimentation rate upcore ($r = 0.71$). In general, the record suggests large rBC fluxes. rBC influx was highest between $\sim 14,500$ and $\sim 14,000$ cal yr BP with maximum values up to $4 \mu\text{g cm}^{-2} \text{y}^{-1}$. Major rBC influx (i.e., a series of influx peaks exceeding $1 \mu\text{g cm}^{-2} \text{y}^{-1}$) also occurred at $\sim 12,000$ to $\sim 11,500$ cal yr BP, ~ 8000 to ~ 7000 cal yr BP, ~ 4000 to ~ 1500 cal yr BP, and ~ 600 cal yr BP to present. Similar to rBC, charcoal influx from Diamond Lake was elevated after ~ 600 cal yr BP (Fig. 6; McWethy et al.,

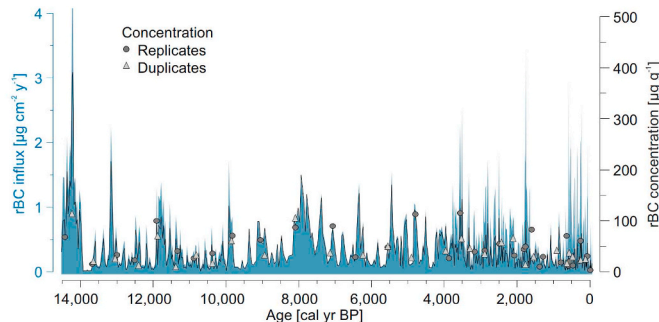


Fig. 2. Refractory black carbon (rBC) record from Diamond Lake spanning 14,000 years. Comparison of rBC concentration (black line) and influx (blue). Point measurements indicate replicate (circles) and duplicate (triangles) concentration measurements in the record.

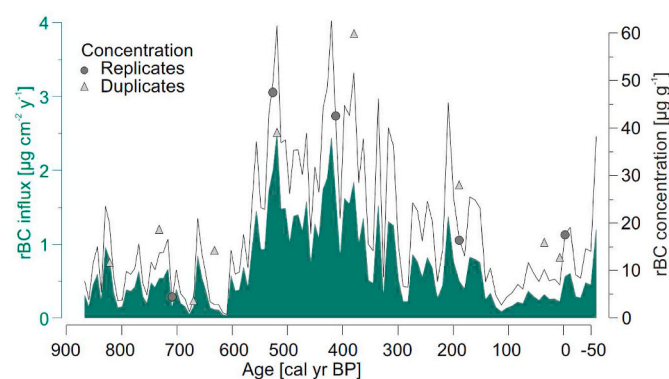


Fig. 3. Refractory black carbon (rBC) record from Horseshoe Lake spanning 900 years. Comparison of rBC concentration (black line) and influx (green). Point measurements indicate replicate (circles) and duplicate (triangles) concentration measurements in the record.

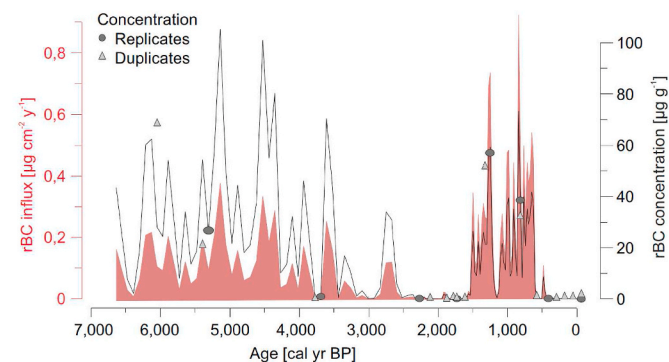


Fig. 4. Refractory black carbon (rBC) record from Lake Rotomānuka spanning 7000 years. Comparison of rBC concentration (black line) and influx (red). Point measurements indicate replicate (circles) and duplicate (triangles) concentration measurements in the record.

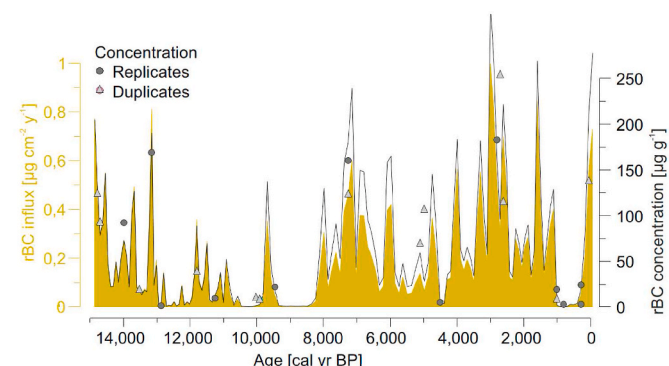


Fig. 5. Refractory black carbon (rBC) record from Lake Kai Iwi spanning 14,000 years. Comparison of rBC concentration (black line) and influx (yellow). Point measurements indicate replicate (circles) and duplicate (triangles) concentration measurements in the record.

2010). However, several periods of enhanced rBC influx prior to ~ 600 cal yr BP were associated with negligible charcoal influx values, resulting in an overall weak correlation ($r = 0.28$) between fire tracers.

rBC concentrations were generally low at Horseshoe Lake, reaching up to $60 \mu\text{g g}^{-1}$ (Fig. 3), and rBC influx followed these trends ($r = 0.99$) over the last ~ 900 years. rBC influx was low ($<1 \mu\text{g cm}^{-2} \text{y}^{-1}$) from ~ 870 to ~ 550 cal yr BP. High rBC influx values (~ 1 – $\sim 4 \mu\text{g cm}^{-2} \text{y}^{-1}$) occurred from ~ 550 to ~ 350 cal yr BP and decreased again to $<1 \mu\text{g}$

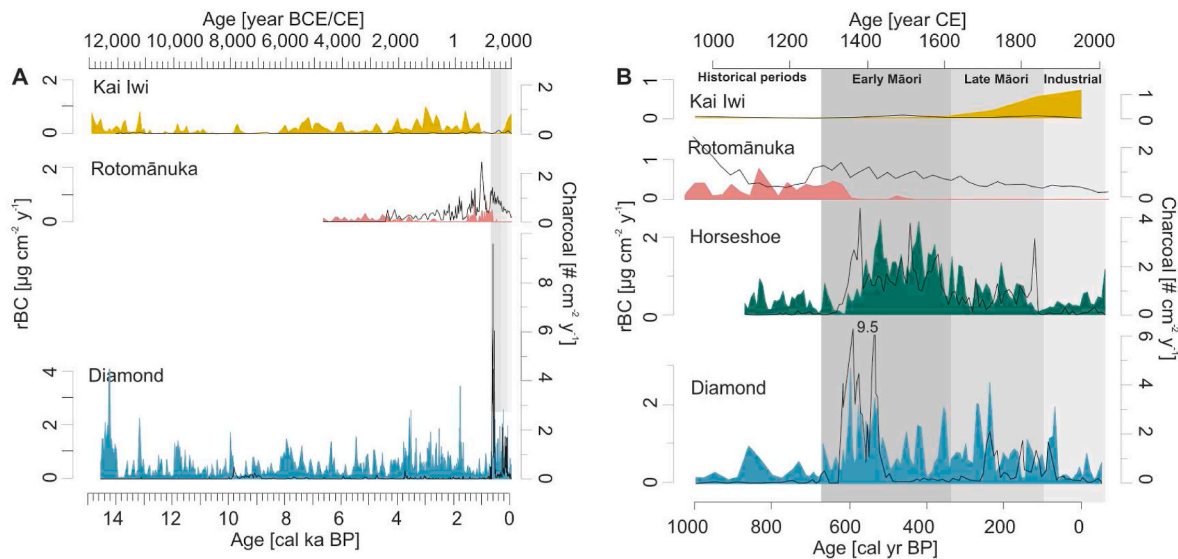


Fig. 6. Comparison of New Zealand burning records in lake sediments. Comparison of refractory black carbon (rBC) and macroscopic charcoal records in New Zealand lake-sediment cores for the Holocene (A) and the last millennium (B). rBC influx is shown as colored curve and charcoal as black line. Note that the Lake Kai Iwi record consists of contiguous sampling, albeit lower resolution due to compacted sediments. The centennial Horseshoe Lake record is only shown in Panel B. Periods of human settlement, at top, following McWethy et al. (2010).

$\text{cm}^{-2} \text{y}^{-1}$ by ~ 150 cal yr BP. After a period of low deposition, rBC influx increased slightly in the recent decades. The charcoal record from Horseshoe Lake suggests a period of almost no charcoal influx before ~ 600 cal yr BP followed by a period of high charcoal deposition (~ 600 – ~ 350 cal yr BP) and low charcoal deposition after ~ 100 cal yr BP (Fig. 6; McWethy et al., 2010). The similar trend and positive correlation between corresponding samples ($r = 0.46$) suggest a shared source area for the rBC and charcoal data.

The ~ 6600 -year-long rBC record from Lake Rotomānuka on the North Island consists of high rBC with concentrations up to $\sim 100 \mu\text{g g}^{-1}$ between ~ 6600 and ~ 3500 cal yr BP and up to $\sim 60 \mu\text{g g}^{-1}$ between ~ 1500 and ~ 500 cal yr BP (Fig. 4). rBC concentrations and influx were extremely low between ~ 2500 and ~ 1500 cal yr BP, and the last ~ 500 years of the record also had values $< 0.1 \mu\text{g g}^{-1}$ and $< 0.001 \mu\text{g cm}^{-2} \text{y}^{-1}$. rBC influx never exceeded $1 \mu\text{g cm}^{-2} \text{y}^{-1}$, which is lower than that of the South Island sites. The rBC influx was slightly elevated between ~ 6600 and ~ 3500 cal yr BP with values up to $\sim 0.4 \mu\text{g cm}^{-2} \text{y}^{-1}$ and was highest ($0.6 \mu\text{g cm}^{-2} \text{y}^{-1}$) from ~ 1500 to ~ 500 cal yr BP. In general, the influx was highest in younger sediments ($< \sim 2500$ cal yr BP to present) whereas concentration values were higher in the older sediments. Differences between concentration and influx levels likely reflect changing sediment accumulation rates (See Appendix C; Fig. S2A). Even the highest rBC peaks at Lake Rotomānuka suggest comparatively little fire activity.

The charcoal record from Lake Rotomānuka is different from that of rBC. Before ~ 4000 cal yr BP, macroscopic charcoal values were mostly below the detection limit, whereas rBC influx values were relatively high (Fig. 6). Charcoal influx increased after 4000 cal yr BP, whereas rBC deposition was minimal from ~ 2500 to 1500 cal yr BP. Similar to the rBC record, charcoal influx reached maximum levels from ~ 1500 to 500 cal yr BP. However, unlike the sharp decrease in rBC influx at ~ 500 cal yr BP to values below the detection limit, the charcoal influx decreased slowly in recent centuries. The differences between the rBC and charcoal record from Lake Rotomānuka ($r = 0.34$) suggest that, similar to Diamond Lake, the two fire proxies reflect different burning source areas and spatial scales.

The northernmost rBC record from Lake Kai Iwi spans the last $\sim 14,800$ years. The temporal resolution of this record was lower than the other records, and low sediment accumulation rates that prevented a detailed interpretation of rBC especially in recent centuries.

Nonetheless, the record provides information on long-term and contiguous background values of rBC. rBC values fluctuated between extremely low ($< 1 \mu\text{g g}^{-1}$) and high concentrations (up to $\sim 250 \mu\text{g g}^{-1}$). rBC influx was similar to the concentration trends with high values from $\sim 14,800$ to $\sim 13,000$ cal yr BP, from ~ 8000 to ~ 1000 cal yr BP, and in the uppermost three samples spanning the last ~ 200 years. Interestingly, rBC influx never exceeded $\sim 1 \mu\text{g cm}^{-2} \text{y}^{-1}$, suggesting that deposition was negligible over the entire Holocene similar to that at Lake Rotomānuka. The charcoal record from Lake Kai Iwi was low over the Holocene suggesting limited fire activity locally (Fig. 6), in agreement with the generally low rBC influx. However, there is no correlation ($r = 0.04$) between rBC and charcoal.

5. Interpretation and discussion

5.1. Holocene sources for rBC deposition in New Zealand lake sediments

rBC concentrations at all four sites with values up to $400 \mu\text{g g}^{-1}$ are in a similar range as previously reported measurements from mid-latitude lake sediment samples of Lake E in Siberia (0 – $\sim 300 \mu\text{g g}^{-1}$) and Island Lake in Wyoming (~ 100 – $\sim 300 \mu\text{g g}^{-1}$; Chellman et al., 2018). They are at the lower end of lake samples from the Amazon basin where values between $300 \mu\text{g g}^{-1}$ and up to $8900 \mu\text{g g}^{-1}$ were recorded with the same methodology (Arienzo et al., 2019).

The contiguous rBC records during the Holocene contrast with charcoal records from all four sites (Lake Diamond, Horseshoe Lake, Lake Rotomānuka, and Lake Kai Iwi) and from other records in New Zealand that have been interpreted as evidence of low fire activity in forest vegetation that rarely burned prior to human arrival (i.e., very few macroscopic charcoal fragments found before the arrival of humans at 1280 McWethy et al., 2010; Perry et al., 2012a; Argiradis et al., 2018; Newnham et al., 2018). rBC particles are two orders of magnitude smaller (Liu et al., 2021) than macroscopic charcoal (Adolf et al., 2018) and some of the rBC particles in the New Zealand records may have come from fires in Australia (e.g., Fig. 7; Butler, 2008; Beck et al., 2017; Mariani et al., 2017, 2019; Adeleye et al., 2021). For example, the Granta Pool record from temperate Tasmania (Fletcher et al., 2014) as well as sites in southeastern Australia at similar latitudes as New Zealand suggest substantial fire activity during the mid-Holocene (e.g., Fig. 7; McKenzie, 1997; Mooney et al., 2011; Abram et al., 2021),

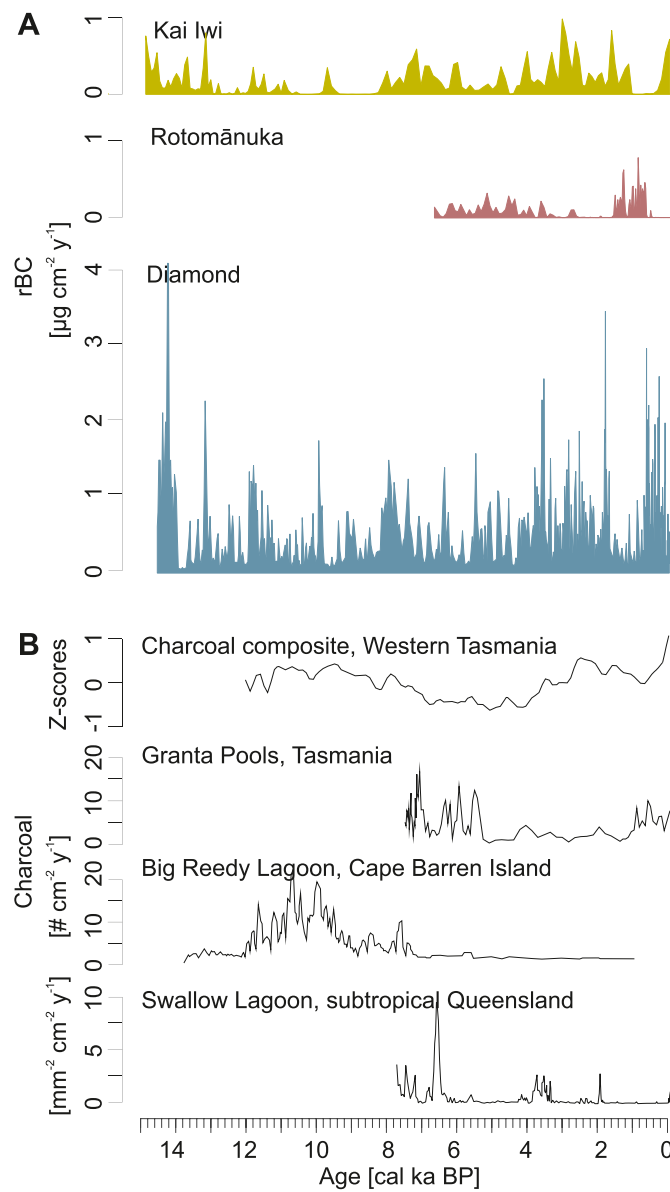


Fig. 7. Comparison of Holocene refractory black carbon (rBC) levels in New Zealand lake sediments with regional charcoal records. Charcoal composite from western Tasmania (Mariani and Fletcher, 2017) and selected sites from western Tasmania (Granta Pools, Fletcher et al., 2014), Cape Barren Island (Adeleye et al., 2021), and subtropical Queensland (Mariani et al., 2019).

contemporaneous with elevated rBC levels at Diamond Lake and Lake Kai Iwi. While charcoal levels at Dove Lake in Tasmania are relatively low throughout the late Holocene, the most prominent fire peak around 4000 cal yr BP (Mariani and Fletcher, 2017) coincides with several large rBC peaks in the Diamond record. A composite record from western Tasmania suggests generally higher fire activity in the early Holocene (Mariani and Fletcher, 2017) that may have produced rBC that could have been transported via the Southern Westerlies to New Zealand, specifically to the South Island site Lake Diamond (and potentially to Lake Rotomānuka, located in the center of North Island). Other records such as the Big Reedy Lagoon record from Cape Barren Island do not show the same pattern as our Holocene rBC records from Lake Diamond, Lake Rotomānuka, and Lake Kai Iwi but it supports substantial fire activity that may have sporadically contributed to New Zealand rBC deposition under suitable atmospheric conditions. In particular, the exposed setting of Lake Kai Iwi on the northwestern coast of the North Island may favor long-distance aerosol input from across the Tasman Sea

and sources from further north with increasing influence of Pacific winds. Previous studies have shown that microscopic charcoal particles up to 20 μm in size and pollen from endemic plants in Australia have been deposited in Lake Kai Iwi sediments (Butler, 2008). For example, the Swallow Lagoon record from subtropical Queensland suggests a major fire peak around 6300 cal yr BP (Mariani et al., 2019) contemporaneous with a period of elevated rBC in the Kai Iwi record (Fig. 7). The possibility of long-distance transport of black carbon aerosols over thousands of kilometers is further supported by FLEXPART atmospheric simulations, which show the potential for black carbon transport over vast areas of the Southern Ocean (Fig. 1). Maritime winds from the Pacific and the Southern Ocean, respectively, allow for considerable rainfall in New Zealand (Howard, 2005) and concomitant wet deposition of particulate matter such as black carbon on South Island that travelled long distances in the atmosphere. While the Westerlies weaken towards northern New Zealand, the North Island lies within the northern edge of the Southern Westerly belt and therefore receives warm maritime air masses from the subtropical Pacific (Shulmeister et al., 2004), which could result in long-range transport of rBC from more northern emission sources. The wet climate in New Zealand with rainfall of 970 mm y^{-1} on the South Island site Horseshoe Lake and up to 1500 mm y^{-1} at Lake Kai Iwi may furthermore favor washout of long-distance rBC in New Zealand and its deposition in the lake catchments in this study.

In addition to long-distance transport contributing to New Zealand rBC records, it is possible that other sources, such as wetland and peat fires on the North Island (Wilmshurst and McGlone, 1996) contributed to the rBC record, although we think this is less likely for two reasons. First, peat fires would have been small and infrequent and unlikely to contribute much rBC (McGlone, 2009). Second, paleoecological data suggest that the peatlands on the South Island did not burn as frequently as those on the North Island (McGlone, 2009), whereas the rBC records from the North Island have lower levels compared to those from the South Island where rBC deposition is orders of magnitudes higher in the Holocene.

Possible low-intensity surface fires of bracken fern and grassland vegetation in the lowlands prevented forest recovery after the Initial Burning Period of the Early Māori period (~ 670 –350 cal yr BP) (Wilmshurst, 1997; Wilmshurst and McGlone, 1996; McWethy et al., 2009, 2014; Holdaway et al., 2019; Prebble et al., 2019). These fires did not produce much macroscopic charcoal (Perry et al., 2012a, 2014) but may have added slightly to the rBC record of the last centuries. In addition, rBC runoff from the lake catchments is limited because the four lakes are closed basins with no inflowing rivers.

In conclusion, it is most likely that fires in Australia (Butler, 2008) contributed to the black carbon detected in New Zealand lake sediments, and depositional differences between the four lakes relate to site-specific transport trajectories and different geographic settings.

5.2. Spatial pattern of rBC deposition levels during different human settlement periods

rBC deposition increased by nearly two-fold on the South Island with the arrival of people, contemporaneous with increased macroscopic charcoal influx. The increase of 0.1 – $3.0 \mu\text{g cm}^{-2} \text{y}^{-1}$ or 1 – $30 \text{ mg m}^{-2} \text{y}^{-1}$; see Fig. 7) is within the expected range of black carbon deposition based on atmospheric modelling at this time (1 – $5 \text{ mg m}^{-2} \text{y}^{-1}$; McConnell et al., 2021). Persistent rBC during the period of human settlement at Diamond Lake and Horseshoe Lake suggests that regional biomass burning lasted beyond the short Initial Burning Period. The sustained rBC increase in New Zealand is contemporaneous with the rBC rise observed in ice-core records from James Ross Island, Antarctica, where rBC persisted long beyond the Initial Burning Period (McConnell et al., 2021). rBC deposition in New Zealand lake sediments was higher during the Early Māori period than the Late Māori period, whereas the Antarctic ice-core records show initially low rBC levels that rise at the start of the Late Māori period about 1600 CE (Newnham, 2022).

The high levels of rBC during the Late Māori period may represent black carbon deposition from both New Zealand and Australian fires. Macroscopic charcoal records from Tasmania indicate rising fire activity (Mariani and Fletcher, 2016) concurrent with the Late Māori period in New Zealand (Newnham, 2022), and these distant fires may have contributed to the prolonged period of high rBC influx on the South Island. Such external sources may explain elevated rBC levels at Diamond Lake when local fire activity, tracked by macroscopic charcoal, declined rapidly after the Initial Burning Period. In contrast, rBC records from the two North Island sites, which had overall low rBC deposition during the period of human settlement, share no common pattern with the South Island sites or Australian records (Fig. 8). The low charcoal levels at both of these sites are also not characteristic of other records from the North Island, such as Lake Pupuke in Auckland, which show a sharp charcoal increase during the human settlement period comparable to the South Island records (Newnham et al., 2018). The highest charcoal levels recorded in any setting in northern New Zealand (Ahuahu) comes from the Early Māori period of occupation on a cultivated wetland, which shows a substantial decline during the Late Māori Period (Prebble et al., 2019). In general, fire patterns on the North Island are spatially more variable than on the South Island due to higher rainfall (Wilmhurst et al., 2008), and pollen and charcoal data indicate that fires were associated with less overall deforestation (estimated to 10–30%) despite higher human populations (Perry et al., 2012b, 2014). The low levels of burning may explain why the two rBC records from the North Island, are relatively homogeneous with low levels.

The contrasted spatial pattern of rBC levels between the South and the North Island records during the period of human settlement may reflect different wind transport pathways across New Zealand. The South Island lies within the northern margin of the Southern Westerlies (Hinojosa et al., 2017; Sturman et al., 1984), which likely transports black carbon from fires in Tasmania to New Zealand as well as to Antarctica (Arienzo et al., 2017; McConnell et al., 2021). The decreased strength of westerly winds towards the northern boundary (Howard, 2005) implies that the North Island fires contributed less to the rBC signal observed in Antarctica.

5.3. Contribution of fossil fuel to the rBC records during the industrial period

rBC decreased at three sites after 1840 CE but not at the northernmost Lake Kai Iwi, where the rBC influx remained low but was elevated in the uppermost two samples compared to the Holocene record. Generally low rBC influx values in the Industrial period agree with charcoal-based fire reconstructions from the same sites. Other charcoal records, however, show initially high levels during the early Industrial

Period (1850 CE to 1900 CE) (McWethy et al., 2010) when approximately 3.3 million hectares of forest were cleared (Perry et al., 2014). However, all four charcoal records in this study suggest relatively low charcoal influx (although higher than the very low Holocene charcoal influx prior to human arrival), thus we infer that the Industrial Period had less influence on biomass burning at our sites than the Initial Burning Period.

rBC deposition from Northern Hemisphere ice cores comes primarily from the burning of fossil fuel during the Industrial Era after ~1850 CE (McConnell et al., 2007; Zennaro et al., 2014; Osmont et al., 2018; Sigl et al., 2018; Eckhardt et al., 2023). Similarly, a rBC record from lake sediments in the Amazon Basin was influenced by fossil fuel emissions during the Industrial Era (Arienzo et al., 2019), and several records of spheroidal carbonaceous fly ash particles (SCP) from Chile, the Falkland Islands (Chirinos et al., 2006; Von Gunten et al., 2009; Rose et al., 2012), Tasmania (Cameron et al., 1993), and an ice core in Antarctica (Thomas et al., 2023) suggest deposition of comparatively large-diameter fossil-fuel-derived particles (micron size) across the Southern Hemisphere, although no record is available from New Zealand itself (Rose, 2015). The first recorded coal deposits in Australia were discovered in 1797 CE, and coal has been mined in New Zealand since the 1840s for domestic use and export (Sherwood and Phillips, 2006; Australian Bureau for Statistics, 2012). Because the rBC records from New Zealand lakes (with the possible exception of Lake Kai Iwi) show no marked increase during the Industrial Era, we interpret them primarily as records of fires. The rBC increase in the northernmost coastal Lake Kai Iwi may derive from fossil fuel burning in Australia (Australian Bureau for Statistics, 2012) or represent regional heathland fires that have occurred frequently in the last decades (Enright, 1989), although further data are needed for confirmation. The overall low rBC deposition in recent decades agrees with Antarctic rBC records, which have little rBC deposition during the Industrial Era (Bisiaux et al., 2012; McConnell et al., 2021; Liu et al., 2021).

Identifying the sources of black carbon during the Industrial Era and disentangling fossil fuel from biomass burning emissions in New Zealand add to knowledge about the atmospheric composition over the Southern Ocean and help interpret rBC records in Antarctica (Liu et al., 2021). Furthermore, identifying the sources of black carbon allows us to understand snow melt associated with the deposition of dark particles in Antarctica as well as on glaciers in New Zealand that currently are threatened by climate warming, prolonged fire seasons, and melting feedbacks (Pu et al., 2021). Such processes will become more prominent in the future as the fire seasons lengthen with further warming. For example, the black carbon deposition from extreme wildfires in Australia in 2019/20 have already resulted in significant post-fire snow darkening in New Zealand and accelerated glacier melt (Pu et al., 2021).

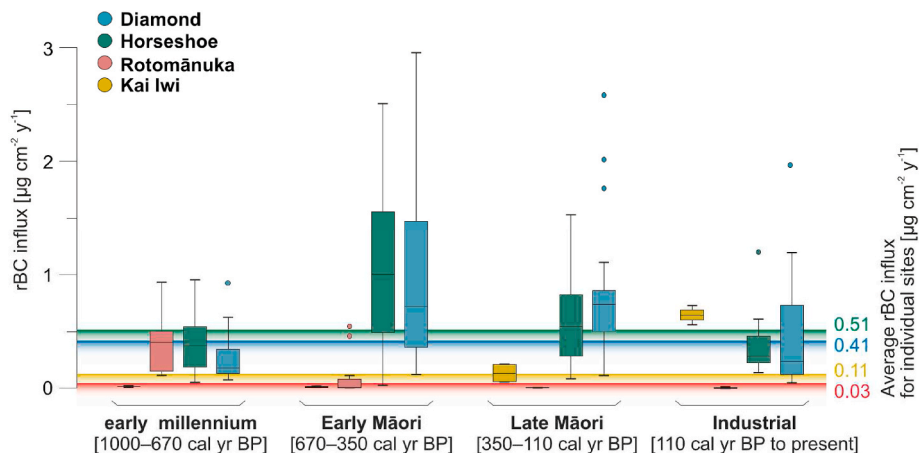


Fig. 8. Refractory black carbon (rBC) levels in New Zealand lake sediments during the human settlement period. Boxplots for rBC influx during the last millennium for each study sites. Horizontal lines indicate average rBC influx over the complete record for each of the sites. Burning periods following McWethy et al. (2010).

6. Conclusions

Our dataset spanning the latitudinal gradient of New Zealand demonstrates the utility of lake-sediment records for understanding the role of regional and local fires in the production and transport of black carbon. First, we conclude that rBC in all four sites probably derived from extra-regional fires including those from Australia. Second, our study suggests that changes in rBC influx through time did not mirror patterns evident in the macroscopic charcoal influx data. We interpret this lack of correspondence to deposition of black carbon sources from distant fires (e.g., Australia) or possibly local peatland fires. Third, when macroscopic charcoal and rBC records match, we interpret this to indicate local fire activity. The increase in rBC after human arrival in 1280 CE coincided with charcoal evidence of extensive fires on the South Island; these fires, along with those in Tasmania, likely contributed to the increase of rBC deposition recorded in Antarctic ice cores. Fourth, rBC deposition in the Industrial Era was low at all four sites in New Zealand, suggesting that anthropogenic disturbance did not increase fire activity during this time.

While these results are intriguing, additional studies comparing rBC with charcoal records across a variety of vegetation types and with atmospheric transport simulations are needed to build an understanding of potential sources of rBC in lake-sediment and ice-cores records. Constraining the sources of black carbon during the Industrial Era by disentangling emissions from fossil fuel versus fires is still needed to better understand the atmospheric black carbon levels over the Southern Ocean and the rBC records in ice cores from Antarctica. rBC records from the New Zealand sites can help constrain the source region for black carbon deposition in New Zealand and provide useful information for evaluating atmospheric transport models. Furthermore, understanding black carbon production and transport from such rBC records will provide insights about the source of dark particles on melting glaciers in New Zealand and Antarctica that are threatened by climate warming.

CRediT authorship contribution statement

Sandra O. Brugger: Conceptualization, Formal analysis, Funding acquisition, Investigation, Visualization, Writing - original draft. **David B. McWethy:** Conceptualization, Formal analysis, Funding acquisition, Investigation, Supervision, Writing - review & editing. **Nathan J. Chellman:** Data curation, Formal analysis, Methodology, Visualization, Writing - review & editing. **Matiu Prebble:** Conceptualization, Validation, Writing - review & editing. **Colin J. Courtney Mustaphi:** Conceptualization, Validation, Writing - review & editing. **Sabine Eckhardt:** Methodology, Writing - review & editing. **Andreas Plach:** Conceptualization, Formal analysis, Writing - review & editing. **Andreas Stohl:** Conceptualization, Supervision, Writing - review & editing. **Janet M. Wilmshurst:** Investigation, Writing - review & editing. **Joseph R. McConnell:** Funding acquisition, Supervision, Writing - review & editing. **Cathy Whitlock:** Conceptualization, Funding acquisition, Supervision, Writing - review & editing, All co-authors approved the final version.

Declaration of competing interest

The authors declare that they have no known competing financial interests or personal relationships that could have appeared to influence the work reported in this paper.

Data availability

Data will be made available on request.

Acknowledgement

We thank Teresa Krause and Jason Baldes for field assistance in the

coreng campaigns at Diamond Lake, Horseshoe Lake, Lake Rotomānuka, and Lake Kai Iwi. Fieldwork was funded by NSF OISE-0966472 and BCS-1024413. rBC measurements were supported by NSF grant 2102917. We thank three anonymous reviewers for their constructive evaluation of our manuscript. This study was funded by the Swiss National Science Foundation SNSF Postdoc. Mobility grant P400P2-199285.

Appendix E. Supplementary data

Supplementary data to this article can be found online at <https://doi.org/10.1016/j.quascirev.2023.108491>.

References

Abram, N.J., Henley, B.J., Sen Gupta, A., Lippmann, T.J., Clarke, H., Dowdy, A.J., Sharples, J.J., Nolan, R.H., Zhang, T., Wooster, M.J., Wurtzel, J.B., Meissner, K.J., Pitman, A.J., Ukkola, A.M., Murphy, B.P., Tapper, N.J., Boer, M.M., 2021. Connections of climate change and variability to large and extreme forest fires in southeast Australia. *Commun. Earth Environ.* 2 (1), 1–17. <https://doi.org/10.1038/s43247-020-00065-8>.

Adeleye, M.A., Haberle, S.G., Harris, S., Hopf, F.V.L., Connor, S., Stevenson, J., 2021. Holocene heathland development in temperate oceanic Southern Hemisphere: key drivers in a global context. *J. Biogeogr.* 48 (5), 1048–1062. <https://doi.org/10.1111/jbi.14057>.

Adolf, C., Wunderle, S., Colombaroli, D., Weber, H., Gobet, E., Heiri, O., van Leeuwen, J. F.N., Bigler, C., Connor, S.E., Galka, M., La Mantia, T., Makhortykh, S., Svitavská-Svobodová, H., Vannière, B., Tinner, W., 2018. The sedimentary and remote-sensing reflection of biomass burning in Europe. *Global Ecol. Biogeogr.* 27 (2), 199–212. <https://doi.org/10.1111/geb.12682>.

Andreae, M.O., Merlet, P., 2001. Emission of trace gases and aerosols from biomass burning. *Global Biogeochem. Cycles* 15 (4), 955–966. <https://doi.org/10.1029/2000GB001382>.

Argiriadis, E., Battistel, D., McWethy, D.B., Vecchiato, M., Kirchgeorg, T., Kehrwald, N. M., Whitlock, C., Wilmshurst, J.M., Barbante, C., 2018. Lake sediment fecal and biomass burning biomarkers provide direct evidence for prehistoric human-lit fires in New Zealand. *Sci. Rep.* 8 (1), 1–9. <https://doi.org/10.1038/s41598-018-30606-3>.

Arienzo, M.M., Maezumi, S.Y., Chellman, N.J., Iriarte, J., 2019. Pre-Columbian fire management linked to refractory black carbon emissions in the Amazon. *Fire* 2 (2), 31. <https://doi.org/10.3390/fire200031>.

Arienzo, M.M., McConnell, J.R., Murphy, L.N., Chellman, N., Das, S., Kipfstuhl, S., Mulvaney, R., 2017. Holocene black carbon in Antarctica paralleled Southern Hemisphere climate. *J. Geophys. Res. Atmos.* 122 (13), 6713–6728. <https://doi.org/10.1002/2017JD026599>.

Australian Bureau for Statistics, 2012. History of Coal Mining. <https://www.abs.gov.au/ausstats/abs@.nsf/featurearticlesbytitle/6893596390A01028CA2569E3001F5555#~:text=Coal%20was%20discovered%20at%20a,up%20the%20coast%20to%20Sydney>.

Beck, K.K., Fletcher, M.S., Gadd, P.S., Heijnis, H., Jacobsen, G.E., 2017. An early onset of ENSO influence in the extra-tropics of the southwest Pacific inferred from a 14,600 year high resolution multi-proxy record from Paddys Lake, northwest Tasmania. *Quat. Sci. Rev.* 157, 164–175. <https://doi.org/10.1016/j.quascirev.2016.12.001>.

Bisiaux, M.M., Edwards, R., McConnell, J.R., Curran, M.A.J., Van Ommen, T.D., Smith, A.M., Neumann, T.A., Pasteris, D.R., Penner, J.E., Taylor, K., 2012. Changes in black carbon deposition to Antarctica from two high-resolution ice core records, 1850–2000 AD. *Atmos. Chem. Phys.* 12 (9), 4107–4115. <https://doi.org/10.5194/acp-12-4107-2012>.

Bond, T.C., Doherty, S.J., Fahey, D.W., Forster, P.M., Berntsen, T., DeAngelo, B.J., Flanner, M.G., Ghan, S., Kärcher, B., Koch, D., Kinne, S., Kondo, Y., Quinn, P.K., Sarofim, M.C., Schultz, M.G., Schulz, Venkataraman, M.C., Zhang, H., Zhang, S., Bellouin, N., Guttikunda, S.K., Hopke, P.K., Jacobson, M.Z., Kaiser, J.W., Klimont, Z., Lohmann, U., Schwarz, J.P., Shindell, D., Storelvmo, T., Warren, S.G., Zender, C.S., 2013. Bounding the role of black carbon in the climate system: a scientific assessment. *J. Geophys. Res. Atmos.* 118 (11), 5380–5552. <https://doi.org/10.1002/jgrd.50171>.

Brugger, S.O., Chellman, N.J., McConnell, C., McConnell, J.R., 2022. High-latitude fire activity of recent decades derived from microscopic charcoal and black carbon in Greenland ice cores. *Holocene*. <https://doi.org/10.1177/09596836221131711>.

Bunbury, M.M., Petchey, F., Bickler, S.H., 2022. A new chronology for the Māori settlement of Aotearoa (NZ) and the potential role of climate change in demographic developments. *Proc. Natl. Acad. Sci. USA* 119 (46), e2207609119. <https://doi.org/10.1073/pnas.2207609119>.

Butler, K., 2008. Interpreting charcoal in New Zealand's palaeoenvironment—what do those charcoal fragments really tell us? *Quat. Int.* 184 (1), 122–128. <https://doi.org/10.1016/j.quaint.2007.09.026>.

Cameron, N.G., Tyler, P.A., Rose, N.L., Hutchinson, S., Appleby, P.G., 1993. The recent palaeolimnology of Lake nicholls, mount field national park, Tasmania. *Hydrobiologia* 269 (1), 361–370. <https://doi.org/10.1007/BF00028035>.

Chatterjee, A., Dutta, M., Ghosh, A., Ghosh, S.K., Roy, A., 2020. Relative role of black carbon and sea-salt aerosols as cloud condensation nuclei over a high altitude urban atmosphere in eastern Himalaya. *Sci. Total Environ.* 742, 140468. <https://doi.org/10.1016/j.scitotenv.2020.140468>.

Chellman, N.J., McConnell, J.R., Heyvaert, A., Vannière, B., Arienzo, M.M., Wennrich, V., 2018. Incandescence-based single-particle method for black carbon quantification in lake sediment cores. *Limnol Oceanogr. Methods* 16 (11), 711–721. <https://doi.org/10.1002/lom3.10276>.

Chirinos, L., Rose, N.L., Urrutia, R., Munoz, P., Torrejón, F., Torres, L., Cruces, F., Araneda, A., Zaror, C., 2006. Environmental evidence of fossil fuel pollution in Laguna Chica de San Pedro lake sediments (Central Chile). *Environ. Pollut.* 141 (2), 247–256. <https://doi.org/10.1016/j.envpol.2005.08.049>.

Eckhardt, S., Pisso, I., Evangelou, N., Zwaftink, C.G., Plach, A., McConnell, J.R., Sigl, M., Ruppel, M., Zdanowicz, C., Lim, S., Chellman, N.J., Opel, T., Meyer, H., Steffensen, J.P., Schwikowski, M., Stohl, A., 2023. Revised historical Northern Hemisphere black carbon emissions based on inverse modeling of ice core records. *Nat. Commun.* 14 (1), 271. <https://doi.org/10.1038/s41467-022-35660-0>.

Enright, N.J., 1989. Heathland vegetation of the Spirits Bay area, far northern New Zealand. *N. Z. J. Ecol.* 63–75. <https://www.jstor.org/stable/24053180>.

Fletcher, M.S., Wood, S.W., Haberle, S.G., 2014. A fire-driven shift from forest to non-forest: evidence for alternative stable states? *Ecology* 95 (9), 2504–2513. <https://doi.org/10.1890/12-1766.1>.

Gustafsson, Ö., Bucheli, T.D., Kukulski, Z., Andersson, M., Largeau, C., Rouzaud, J.N., Reddy, C.M., Eglinton, T.I., 2001. Evaluation of a protocol for the quantification of black carbon in sediments. *Global Biogeochem. Cycles* 15 (4), 881–890. <https://doi.org/10.1029/2000GB001380>.

Hamilton, D.S., Hantson, S., Scott, C.E., Kaplan, J.O., Pringle, K.J., Nieradzik, L.P., Rap, A., Folberth, G.A., Spracklen, Carslaw, K.S., 2018. Reassessment of pre-industrial fire emissions strongly affects anthropogenic aerosol forcing. *Nat. Commun.* 9 (1), 1–12. <https://doi.org/10.1038/s41467-018-05592-9>.

Han, Y.M., Cao, J.J., Yan, B.Z., Kenna, T.C., Jin, Z.D., Cheng, Y., Chow, J.C., An, Z.S., 2011. Comparison of elemental carbon in lake sediments measured by three different methods and 150-year pollution history in eastern China. *Environ. Sci. Technol.* 45 (12), 5287–5293. <https://doi.org/10.1021/es103518c>.

Hartmann, M., Blunier, T., Brugger, S.O., Schmale, J., Schwikowski, M., Vogel, A., Wex, H., Stratmann, F., 2019. Variation of ice nucleating particles in the European Arctic over the last centuries. *Geophys. Res. Lett.* 46 (7), 4007–4016. <https://doi.org/10.1029/2019GL082311>.

Hinojosa, J.L., Moy, C.M., Stirling, C.H., Wilson, G.S., Eglinton, T.I., 2017. A New Zealand perspective on centennial-scale Southern Hemisphere westerly wind shifts during the last two millennia. *Quat. Sci. Rev.* 172, 32–43. <https://doi.org/10.1016/j.quascirev.2017.07.016>.

Hogg, A.G., Heaton, T.J., Hua, Q., Palmer, J.G., Turney, C.S., Southon, J., Bayliss, A., Blackwell, P.G., Boswijk, G., Ramsey, C.B., Pearson, C., Petley, F., Reimer, P., Reimer, R., Wacker, L., 2020. SHCal20 Southern Hemisphere calibration, 0–55,000 years cal BP. *Radiocarbon* 62 (4), 759–778. <https://doi.org/10.1017/RDC.2020.59>.

Holdaway, S.J., Emmitt, J., Furey, L., Jorgensen, A., O'Regan, G., Phillipps, R., Prebble, M., Wallace, R., Ladefoged, T.N., 2019. Māori settlement of New Zealand: the Anthropocene as a process. *Archaeol. Ocean.* 54 (1), 17–34. <https://doi.org/10.1002/arc0.5173>.

Howard, A., 2005. Australia and New Zealand, climate of. In: Oliver, J.E. (Ed.), *Encyclopedia of World Climatology. Encyclopedia of Earth Sciences Series*. Springer, Dordrecht, pp. 137–154. https://doi.org/10.1007/1-4020-3266-8_26.

Kruger, B.R., Hausner, M.B., Chellman, N., Weaver, M., Samburova, V., Khlystov, A., 2023. Dissolved black carbon as a potential driver of surface water heating dynamics in wildfire-impacted regions: a case study from Pyramid Lake, NV, USA. *Sci. Total Environ.* 888, 164141. <https://doi.org/10.1016/j.scitotenv.2023.164141>.

Leathwick, J., Wilson, G., Rutledge, D., Wardle, P., Morgan, F., Johnston, K., McLeod, M., Kirkpatrick, R., 2003. *Land Environments of New Zealand*. David Bateman Ltd., Auckland.

Li, F., Val Martin, M., Andreae, M.O., Arneth, A., Hantson, S., Kaiser, J.W., Lasslop, G., Yue, C., Bachelet, D., Forrest, M., Kluzek, E., Liu, X., Mangeon, S., Melton, J.R., Ward, D.S., Darmenov, A., Hickler, T., Ichoku, C., Magi, B.I., Sitch, S., van der Werf, G.R., Wiedinmyer, C., Rabin, S.S., 2019. Historical (1700–2012) global multi-model estimates of the fire emissions from the fire modeling intercomparison project (FireMIP). *Atmos. Chem. Phys.* 19 (19), 12545–12567. <https://doi.org/10.5194/acp-19-12545-2019>.

Li, H., Lamb, K.D., Schwarz, J.P., Selimovic, V., Yokelson, R.J., McMeeking, G.R., May, A.A., 2019. Inter-comparison of black carbon measurement methods for simulated open biomass burning emissions. *Atmos. Environ.* 206, 156–169. <https://doi.org/10.1016/j.atmosenv.2019.03.010>.

Liu, P., Kaplan, J.O., Mickley, L.J., Li, Y., Chellman, N.J., Arienzo, M.M., Kodros, J.K., Sigl, M., Freitag, J., Mulvaney, R., Curran, M.A.J., McConnell, J.R., 2021. Improved estimates of preindustrial biomass burning reduce the magnitude of aerosol climate forcing in the Southern Hemisphere. *Sci. Adv.* 7 (22), eabc1379. <https://doi.org/10.1126/sciadv.abc1379>.

Mariani, M., Fletcher, M.S., 2016. The Southern Annular Mode determines interannual and centennial-scale fire activity in temperate southwest Tasmania, Australia. *Geophys. Res. Lett.* 43 (4), 1702–1709. <https://doi.org/10.1002/2016GL068082>.

Mariani, M., Connor, S.E., Fletcher, M.S., Theuerkauf, M., Kunes, P., Jacobsen, G., Saunders, K.M., Zawadzki, A., 2017. How old is the Tasmanian cultural landscape? A test of landscape openness using quantitative land-cover reconstructions. *J. Biogeogr.* 44 (10), 2410–2420. <https://doi.org/10.1111/jbi.13040>.

Mariani, M., Fletcher, M.S., 2017. Long-term climate dynamics in the extra-tropics of the South Pacific revealed from sedimentary charcoal analysis. *Quat. Sci. Rev.* 173, 181–192. <https://doi.org/10.1016/j.quascirev.2017.08.007>.

Mariani, M., Tibby, J., Barr, C., Moss, P., Marshall, J.C., McGregor, G.B., 2019. Reduced rainfall drives biomass limitation of long-term fire activity in Australia's subtropical sclerophyll forests. *J. Biogeogr.* 46 (9), 1974–1987. <https://doi.org/10.1111/jbi.13628>.

Marlon, J.R., 2020. What the past can say about the present and future of fire. *Quat. Res.* 96, 66–87. <https://doi.org/10.1017/qua.2020.48>.

McConnell, J.R., Chellman, N.J., Mulvaney, R., Eckhardt, S., Stohl, A., Plunkett, G., Kipfstuhl, S., Freitag, J., Isaksson, E., Gleason, K.E., Brugger, S.O., McWethy, D.B., Abram, N.J., Liu, P., Aristarain, A.J., 2021. Hemispheric black carbon increase after the 13th-century Māori arrival in New Zealand. *Nature* 598 (7879), 82–85. <https://doi.org/10.1038/s41586-021-03858-9>.

McConnell, J.R., Edwards, R., Kok, G.L., Flanner, M.G., Zender, C.S., Saltzman, E.S., Banta, J.R., Pasteris, D.R., Carter, M.M., Kahl, J.D., 2007. 20th-century industrial black carbon emissions altered arctic climate forcing. *Science* 317 (5843), 1381–1384. <https://doi.org/10.1126/science.11448>.

McGlone, M.S., Wilmshurst, J.M., 1999. Dating initial Māori environmental impact in New Zealand. *Quat. Int.* 59 (1), 5–16. [https://doi.org/10.1016/S1040-6182\(98\)00067-6](https://doi.org/10.1016/S1040-6182(98)00067-6).

McGlone, M.S., 2009. Postglacial history of New Zealand wetlands and implications for their conservation. *N. Z. J. Ecol.* 1–23. <https://www.jstor.org/stable/24060858>.

McKenzie, G.M., 1997. The late Quaternary vegetation history of the south-central highlands of Victoria, Australia. I. Sites above 900 m. *Aust. J. Ecol.* 22 (1), 19–36. <https://doi.org/10.1111/j.1442-9993.1997.tb00638.x>.

McWethy, D.B., Whitlock, C., Wilmshurst, J.M., McGlone, M.S., Fromont, M., Li, X., Diefenbacher-Krall, A., Hobbs, W.O., Fritz, S.C., Cook, E.R., 2010. Rapid landscape transformation in South Island, New Zealand, following initial Polynesian settlement. *Proc. Natl. Acad. Sci. USA* 107 (50), 21343–21348. <https://doi.org/10.1073/pnas.1011801107>.

McWethy, D.B., Whitlock, C., Wilmshurst, J.M., McGlone, M.S., Li, X., 2009. Rapid deforestation of south island, New Zealand, by early Polynesian fires. *Holocene* 19 (6), 883–897. <https://doi.org/10.1177/0959683609336563>.

McWethy, D.B., Wilmshurst, J.M., Whitlock, C., Wood, J.R., McGlone, M.S., 2014. A high-resolution chronology of rapid forest transitions following Polynesian arrival in New Zealand. *PLoS One* 9 (11), e111328. <https://doi.org/10.1371/journal.pone.0111328>.

Mooney, S.D., Harrison, S.P., Bartlein, P.J., Daniau, A.L., Stevenson, J., Brownlie, K.C., Buckman, S., Cupper, M., Luly, J., Black, M., Colhoun, E., D'Costa, D., Dodson, J., Haberle, S., Hope, G.S., Kershaw, P., Kenyon, C., McKenzie, M., Williams, N., 2011. Late quaternary fire regimes of Australasia. *Quat. Sci. Rev.* 30 (1–2), 28–46. <https://doi.org/10.1016/j.quascirev.2010.10.010>.

Motos, G., Schmale, J., Corbin, J.C., Modini, R., Karlen, N., Bertò, M., Baltensperger, U., Gysel-Beer, M., 2019. Cloud droplet activation properties and scavenged fraction of black carbon in liquid-phase clouds at the high-alpine research station Jungfraujoch (3580 m asl). *Atmos. Chem. Phys.* 19 (6), 3833–3855. <https://doi.org/10.5194/acp-19-3833-2019>.

Newnham, R.M., 2022. Black carbon attribution. *Nature* 612 (7941), E18–E19. <https://doi.org/10.1038/s41586-022-05518-y>.

Newnham, R.M., Alloway, B.V., Holt, K.A., Butler, K., Rees, A.B.H., Wilmshurst, J.M., Dunbar, G., Hajdas, I., 2017. Last Glacial pollen-climate reconstructions from Northland, New Zealand. *J. Quat. Sci.* 32 (6), 685–703. <https://doi.org/10.1002/jqs.2955>.

Newnham, R.M., Lowe, D.J., Green, J.D., 1989. Palynology, vegetation and climate of the Waikato lowlands, North Island, New Zealand since c. 18,000 years ago. *J. Roy. Soc. N. Z.* 19 (2), 127–150. <https://doi.org/10.1080/03036758.1989.10426443>.

Newnham, R., Lowe, D.J., Gehrels, M., Augustinus, P., 2018. Two-step human-environmental impact history for northern New Zealand linked to late-Holocene climate change. *Holocene* 28 (7), 1093–1106. <https://doi.org/10.1177/0959683618761545>.

Novakov, T., Ramanathan, V., Hansen, J.E., Kirchstetter, T.W., Sato, M., Sinton, J.E., Sathaye, J.A., 2003. Large historical changes of fossil-fuel black carbon aerosols. *Geophys. Res. Lett.* 30 (6) <https://doi.org/10.1029/2002GL016345>.

Ohata, S., Moteki, N., Schwarz, J., Fahey, D., Kondo, Y., 2013. Evaluation of a method to measure black carbon particles suspended in rainwater and snow samples. *Aerosol Sci. Technol.* 47 (10), 1073–1082. <https://doi.org/10.1080/0278626.2013.824067>.

Osmont, D., Sigl, M., Eichler, A., Jenk, T.M., Schwikowski, M., 2019. A Holocene black carbon ice-core record of biomass burning in the Amazon Basin from Illimani, Bolivia. *Clim. Past* 15 (2), 579–592. <https://doi.org/10.5194/cp-15-579-2019>.

Osmont, D., Wendl, I.A., Schmidely, L., Sigl, M., Vega, C.P., Isaksson, E., Schwikowski, M., 2018. An 800-year high-resolution black carbon ice core record from Lomonosovfonna, Svalbard. *Atmos. Chem. Phys.* 18 (17), 12777–12795. <https://doi.org/10.5194/acp-18-12777-2018>.

Osmont, D., Brugger, S., Gilgen, A., Weber, H., Sigl, M., Modini, R.L., Schwoerer, C., Tinner, W., Wunderle, S., Schwikowski, M., 2020. Tracing devastating fires in Portugal to a snow archive in the Swiss Alps: a case study. *Cryosphere* 14 (11), 3731–3745. <https://doi.org/10.5194/tc-14-3731-2020>.

Page, M.J., Trustrum, N.A., DeRose, R.C., 1994. A high resolution record of storm-induced erosion from lake sediments, New Zealand. *J. Paleolimnol.* 11, 333–348. <https://doi.org/10.1007/BF00677993>.

Pearson, L.K., 2007. The Nature, Composition and Distribution of Sediment in Lake Rotorua, New Zealand (Thesis, Master of Science (MSc)). The University of Waikato, Hamilton, New Zealand. <https://hdl.handle.net/10289/2333>.

Perry, G.L., Wilmshurst, J.M., McGlone, M.S., 2014. Ecology and long-term history of fire in New Zealand. *N. Z. J. Ecol.* 157–176. <https://www.jstor.org/stable/24060795>.

Perry, G.L., Wilmshurst, J.M., McGlone, M.S., Napier, A., 2012b. Reconstructing spatial vulnerability to forest loss by fire in pre-historic New Zealand. *Global Ecol. Biogeogr.* 21 (10), 1029–1041. <https://doi.org/10.1111/j.1466-8238.2011.00745.x>.

Perry, G.L., Wilmshurst, J.M., McGlone, M.S., McWethy, D.B., Whitlock, C., 2012a. Explaining fire-driven landscape transformation during the Initial Burning Period of

New Zealand's prehistory. *Global Change Biol.* 18 (5), 1609–1621. <https://doi.org/10.1111/j.1365-2486.2011.02631.x>.

Pisso, I., Sollum, E., Grythe, H., Kristiansen, N.I., Cassiani, M., Eckhardt, S., Arnold, D., Morton, D., Thompson, R.J., Groot Zwaaftink, C.D., Evangelou, N., Sodemann, H., Haimberger, L., Henne, S., Brunner, D., Burkhardt, J.F., Fouilloux, A., Brioude, J., Philipp, A., Seibert, P., Stohl, A., 2019. The Lagrangian particle dispersion model FLEXPART version 10.4. *Geosci. Model Dev. (GMD)* 12 (12), 4955–4997. <https://doi.org/10.5194/gmd-12-4955-2019>.

Prebble, M., Anderson, A.J., Augustinus, P., Emmitt, J., Fallon, S.J., Furey, L.L., Holdaway, S.J., Jorgensen, A., Ladefoged, T.N., Matthews, P.J., Meyer, J.-Y., Phillipps, R., Wallace, R., Porch, N., 2019. Early tropical crop production in marginal subtropical and temperate Polynesia. *Proc. Natl. Acad. Sci. USA* 116 (18), 8824–8833. <https://doi.org/10.1073/pnas.1821732116>.

Pu, W., Cui, J., Wu, D., Shi, T., Chen, Y., Xing, Y., Zhou, Y., Wang, X., 2021. Unprecedented snow darkening and melting in New Zealand due to 2019–2020 Australian wildfires. *Fundam. Res.* 1 (3), 224–231. <https://doi.org/10.1016/j.fmre.2021.04.001>.

Rose, N.L., 2015. Spheroidal carbonaceous fly ash particles provide a globally synchronous stratigraphic marker for the Anthropocene. *Environ. Sci. Technol.* 49 (7), 4155–4162. <https://doi.org/10.1021/acs.est.5b00543>.

Rose, N.L., Jones, V.J., Noon, P.E., Hodgson, D.A., Flower, R.J., Appleby, P.G., 2012. Long-range transport of pollutants to the Falkland Islands and Antarctica: evidence from lake sediment fly ash particle records. *Environ. Sci. Technol.* 46 (18), 9881–9889. <https://doi.org/10.1021/es3023013>.

Ruppel, M.M., Eckhardt, S., Pesonen, A., Mizohata, K., Oinonen, M.J., Stohl, A., Anderson, A., Jones, V., Manninen, S., Gustafsson, O., 2021. Observed and modeled black carbon deposition and sources in the Western Russian Arctic 1800–2014. *Environ. Sci. Technol.* 55 (8), 4368–4377. <https://doi.org/10.1021/acs.est.0c07656>.

Schwarz, J.P., Spackman, J.R., Fahey, D.W., Gao, R.S., Lohmann, U., Stier, P., Watts, L.A., Thomson, D.S., Lack, D.A., Pfister, L., Mahoney, M.J., Baumgardner, D., Wilson, D., Reeves, J.M., 2008. Coatings and their enhancement of black carbon light absorption in the tropical atmosphere. *J. Geophys. Res. Atmos.* 113 (D3) <https://doi.org/10.1029/2007JD009042>.

Schwarz, J.P., Gao, R.S., Perring, A.E., Spackman, J.R., Fahey, D.W., 2013. Black carbon aerosol size in snow. *Sci. Rep.* 3 (1), 1356. <https://doi.org/10.1038/srep01356>.

Sherwood, A., Phillips, J., 2006. Coal and Coal Mining, Te Ara - the Encyclopedia of New Zealand. <http://www.TeAra.govt.nz/en/coal-and-coal-mining>. (Accessed 22 November 2022).

Shulmeister, J., Goodwin, I., Renwick, J., Harle, K., Armand, L., McGlone, M.S., Cook, E., Dodson, J., Hesse, P.P., Mayewski, P., Curran, M., 2004. The Southern Hemisphere westerlies in the Australasian sector over the last glacial cycle: a synthesis. *Quat. Int.* 118, 23–53. [https://doi.org/10.1016/S1040-6182\(03\)00129-0](https://doi.org/10.1016/S1040-6182(03)00129-0).

Sigl, M., Abram, N.J., Gabrieli, J., Jenk, T.M., Osmont, D., Schwikowski, M., 2018. 19th century glacier retreat in the Alps preceded the emergence of industrial black carbon deposition on high-alpine glaciers. *Cryosphere* 12 (10), 3311–3331. <https://doi.org/10.5194/tc-12-3311-2018>.

Stohl, A., Forster, C., Frank, A., Seibert, P., Wotawa, G., 2005. The Lagrangian particle dispersion model FLEXPART version 6.2. *Atmos. Chem. Phys.* 5 (9), 2461–2474. <https://doi.org/10.5194/acp-5-2461-2005>.

Sturman, A.P., Trewniard, A.C., Gorman, P.A., 1984. A study of atmospheric circulation over the South Island of New Zealand (1961–1980). *Weather Clim.* 4 (2), 53–62. <https://doi.org/10.2307/44279622>.

Thomas, E.R., Vladimirova, D.O., Tetzner, D.R., Emanuelsson, D.B., Humby, J., Turner, S.D., Rose, N.L., Roberts, S.L., Gaca, P., Cundy, A.B., 2023. The palmer ice core as a candidate global boundary stratotype section and point for the anthropocene series. *Anthropol. Rev.* <https://doi.org/10.1177/20530196231155191>.

Van Marle, M.J., Kloster, S., Magi, B.I., Marlon, J.R., Daniau, A.L., Field, R.D., Arneth, A., Forrest, M., Hantson, S., Kehrwald, N.M., Knorr, W., Lasslop, G., Li, F., Mangeon, S., Yue, C., Kaiser, J.W., van der Werf, G.R., 2017. Historic global biomass burning emissions for CMIP6 (BB4CMIP) based on merging satellite observations with proxies and fire models (1750–2015). *Geosci. Model Dev. (GMD)* 10 (9), 3329–3357. <https://doi.org/10.5194/gmd-10-3329-2017>.

Von Gunten, L., Grosjean, M., Beer, J., Grob, P., Morales, A., Urrutia, R., 2009. Age modeling of young non-varved lake sediments: methods and limits. Examples from two lakes in Central Chile. *J. Paleolimnol.* 42 (3), 401–412. <https://doi.org/10.1007/s10933-008-9284-5>.

Watts, T., Brugger, S.O., 2022. Paleofire data for public health nursing wildfire planning: a planetary perspective. *Am. J. Publ. Health* 112 (S3), 241–244. <https://doi.org/10.2105/AJPH.2022.306760>.

Whitlock, C., Larsen, C., 2002. Charcoal as a fire proxy. In: Smol, J.P., Birks, H.J., Last, W.M. (Eds.), *Tracking Environmental Change Using Lake Sediments: Volume 3: Terrestrial, Algal, and Siliceous Indicators*, vol. 3. Springer, Dordrecht, pp. 75–97. https://doi.org/10.1007/0-306-47668-1_5.

Whitlock, C., Millspaugh, S.H., 1996. Testing the assumptions of fire-history studies: an examination of modern charcoal accumulation in Yellowstone National Park, USA. *Holocene* 6 (1), 7–15. <https://doi.org/10.1177/095968369600600102>.

Wilmshurst, J.M., 1997. The impact of human settlement on vegetation and soil stability in Hawke's Bay, New Zealand. *N. Z. J. Bot.* 35 (1), 97–111. <https://doi.org/10.1080/0028825X.1997.10410672>.

Wilmshurst, J.M., Anderson, A.J., Higham, T.F., Worthy, T.H., 2008. Dating the late prehistoric dispersals of Polynesians to New Zealand using the commensal Pacific rat. *Proc. Natl. Acad. Sci. USA* 105 (22), 7676–7680. <https://doi.org/10.1073/pnas.0801507105>.

Wilmshurst, J.M., McGlone, M.S., 1996. Forest disturbance in the central North Island, New Zealand, following the 1850 BP Taupo eruption. *Holocene* 6 (4), 399–411. <https://doi.org/10.1177/095968369600600402>.

Wood, J.R., Wilmshurst, J.M., Newman, R.N., McGlone, M.S., 2017. Evolution and ecological change during the New Zealand quaternary. In: Shulmeister, J. (Ed.), *Landscape and Quaternary Environmental Change in New Zealand*. Atlantis Press, Paris, pp. 235–291.

Zennaro, P., Kehrwald, N., McConnell, J.R., Schüpbach, S., Maselli, O.J., Marlon, J., Valletonga, P., Leuenberger, D., Zangrandi, R., Spolaor, A., Borroto, M., Barbaro, E., Gambaro, A., Barbante, C., 2014. Fire in ice: two millennia of boreal forest fire history from the Greenland NEEM ice core. *Clim. Past* 10 (5), 1905–1924. <https://doi.org/10.5194/cp-10-1905-2014>.